

Exploiting Protein Conformational Change to Optimize Adenosine-Derived Inhibitors of HSP70

*Matthew D. Cheeseman, Isaac Westwood, Olivier Barbeau, Martin Rowlands, Alan Jones, Fiona Jeganathan, Rosemary Burke, Sarah Dobson, Paul Workman, Ian Collins, Rob van Montfort, Keith Jones**

Cancer Research UK Cancer Therapeutics Unit at The Institute of Cancer Research, London SW7 3RP, U.K.

KEYWORDS HSP70, inhibitors, adenosine, nucleoside, nucleotide, conformation.

ABSTRACT

HSP70 is a molecular chaperone and a key component of the heat shock response. Due to its proposed importance in oncology, this protein has become a popular target for drug discovery efforts, efforts which have as yet brought little success. In this study, we have demonstrated that adenosine derived HSP70 inhibitors bind to the protein with a novel mechanism of action, the stabilization by desolvation of an intramolecular salt-bridge, which induces a conformational change in the protein, leading to high affinity ligands. We also demonstrate that through the

application of this mechanism, adenosine derived HSP70 inhibitors can be optimized in a rational manner.

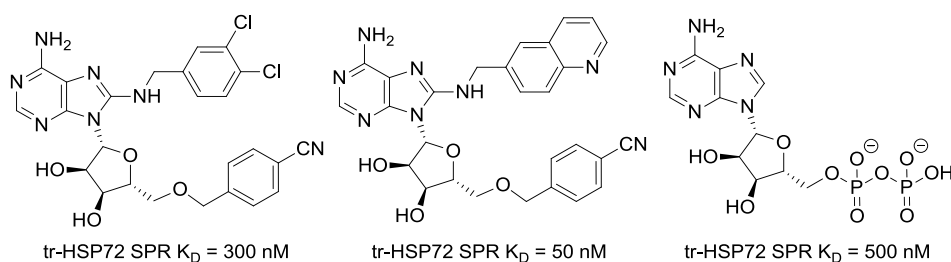
INTRODUCTION

Heat shock proteins are a highly conserved family of molecular chaperones that facilitate the folding, stability and cellular localization of their substrate proteins.¹ Up-regulation of the pathways associated with the heat shock response has been implicated in a number of disease areas, including cancer.² Recent focus has been on the inhibition of the molecular chaperone HSP90 using ATP-competitive inhibitors, an approach that has resulted in considerable success as several compounds have now entered clinical trials.³ The HSP70 family of molecular chaperones represents another potential target for small-molecule mediated antagonism of the heat-shock response pathway. The HSP70 isoform HSC70 is ubiquitously expressed in most tissues, whilst the inducible isoform HSP72 is largely expressed in response to stress, including treatment with HSP90 inhibitors, and aids cell survival through inhibition of several apoptotic pathways.⁴ We have previously shown that dual knockdown of these two HSP70 isoforms in human colon and ovarian tumor cell lines results in apoptosis, which was in contrast with non-tumorigenic cell lines where apoptosis was not observed, indicating a potential therapeutic window for HSP70 inhibitors.⁵

In order to execute their refolding activity, the HSP70 proteins utilize the hydrolysis of ATP to ADP/P_i in a complex catalytic cycle involving a number of protein conformational changes and through a process which is tightly regulated by various co-chaperones.⁶ While this complexity presents numerous opportunities to antagonize the refolding activity of HSP70, the clearest strategy remains ATP-competitive binding of inhibitors to the conserved nucleotide binding domain of the protein. Unfortunately, this approach has proven particularly challenging. There

remains only one published chemotype which displays ATP-competitive sub-micromolar inhibition of HSP70 and has been shown to be effective in cellular assays, a chemotype derived from adenosine(Figure 1).^{7,8}

Figure 1. Adenosine-derived ATP-competitive inhibitors of HSP70



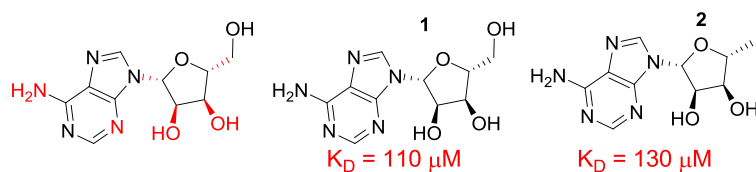
The ATPase domain of HSP70 is a member of the actin ATPase family of proteins, a target class which has delivered very little success in the discovery of high affinity ligands.⁹ A recent study¹⁰ to assess the potential of the HSP70 ATP binding site for antagonism with small molecules using SiteMap^{®11} described the target as “difficult”;¹² whilst a separate analysis using a fragment-based screening approach returned a very low hit rate (0.4%),¹⁰ a result generally associated with low ligandability.¹³ Also, several studies into the biochemical mechanism of HSP70 refolding activity and ATP hydrolysis have demonstrated that the ATP binding site of HSP70 in solution is highly flexible in nature, undergoing numerous conformational changes.¹⁴

With the challenge of finding ATP-competitive hit matter against HSP70 hindering the potential development of inhibitors for this important target, we sought to investigate the binding mechanism of adenosine-derived ligands to the ATP site of HSP70. The aim was to improve our understanding of how high affinity ligands bind to this region of the protein so that this knowledge could be applied to future inhibitor design.

DEVELOPMENT OF TOYOCAMYCIN DERIVED LIGANDS

The slow turnover of ATP by HSP70 and the potent product inhibition by ADP/P_i¹⁵ means that functional assays are challenging for the development inhibitors with this protein. Therefore, we focused on using surface plasmon resonance (SPR) as a biophysical method to assess the affinity of ligands. Unfortunately, full-length human HSP70 gave poor SPR data in our hands. Therefore, the nucleotide-binding domain (NBD) of human HSC70 (tr-HSC70 residues 1 to 381)¹⁶ was used in all SPR experiments. Adenosine **1** is a relatively weak ligand for tr-HSC70, displaying a pK_D = 3.95±0.01 (K_D = 110 μM, n = 3),¹⁷ when measured by SPR, but we decided to use this compound as a starting point for our investigations into the binding mechanisms of this chemotype to the HSP70 proteins. We began by analyzing the importance of the ribose motif to the binding affinity of adenosine **1**. Removing either the 2'- or 3'-hydroxyl groups¹⁸ from the sugar motif or changing their relative and absolute stereochemistry resulted in no measurable binding being observed with concentrations up to 1 mM (data not shown, see supporting information). Removal of either the 6-amino group or the 3-nitrogen of adenine ring also resulted in the loss of all measurable activity. These results demonstrated the importance of the ribose motif and the adenine aminopyrimidine motif to binding of adenosine-derived ligands to the hydrophilic region of the protein. In contrast, removal of the 5'-hydroxyl was well tolerated, as compound **2** retained its activity in with a pK_D = 3.88±0.02 (K_D = 130 μM, n = 3) (Figure 2 and SI Table 1).¹⁹

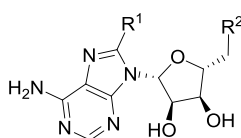
Figure 2. The 5'-ribose hydroxyl has little effect on affinity



The heteroatoms and stereo chemistry highlighted in red are important for affinity to HSP70 and could not be replaced by hydrogen or CH or the stereochemistry changed.

It had previously been shown by Massey *et al* that addition of a primary or secondary amine to the 8-position of adenosine resulted in a significant increase in affinity for these ligands.⁷ In our hands, 8-aminoadenosine **3** gave a $pK_D = 5.16 \pm 0.01$ ($K_D = 7.0 \mu\text{M}$, $n = 3$) a 16-fold increase in affinity when compared to adenosine **1**. We decided to investigate this substituent in order to better understand its role in the improved affinity of these compounds (Table 1).

Table 1. 8- and 5'-Substituted adenosine based HSP70 ligands



Entry	Compd.	R ¹	R ²	$pK_D \pm \text{SEM}^a$	$K_D (\mu\text{M})^b$
1	3			5.16 ± 0.01	7.0
2	4			4.77 ± 0.02	17
3	5			<3.00	>1000
4	6			<3.00	>1000
5	7			4.56 ± 0.01	27

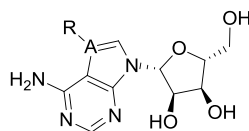
^aAll results are quoted as the geometric mean \pm SEM of 3 independent experiments unless otherwise stated, $pK_D = -\log_{10}(K_D(\mu\text{M}) * 10^{-6})$. ^bAll values are quoted to 2 significant figures.

Methyl substitution on the 8-amino group (entry 2) gave ligand **4** and resulted in a 2.5-fold drop in affinity,²⁰ while dimethyl analogue **5** (entry 3) displayed a K_D greater than 1 mM. Replacement of the 8-amino substituent with a methoxy group to give **6** (entry 4) also resulted in a complete loss of activity. This dramatic effect on binding suggested that one of the hydrogens of the 8-amino group was involved in hydrogen bonding. To assess whether an intramolecular hydrogen bond to the 5'-hydroxyl was important for affinity we removed this group to give **7**

(entry 5). However, only a 4-fold drop affinity was observed with analogue **7** when compared with 8-aminoadenosine **3**, and **7** still displays a 4-fold increase in affinity when compared to adenosine **1**. These results indicate that an intramolecular hydrogen bond between the 8-amino substituent and the 5'-hydroxyl group cannot completely explain the increased affinity observed with the 8-aminoadenosine series when compared with adenosine analogues or the observed activity cliff when both hydrogen bond donors are blocked.²¹

Finally, we sought to investigate the role of the imidazole ring of adenosine to the binding of these ligands to HSP70 (Table 2).

Table 2. Natural product nucleoside derived HSP70 ligands



Entry	Compd.	Name ^a	R	A	pK _D ±SEM ^b	K _D (μM) ^c
1	1	Adenosine	H	N	3.95±0.01	110
2	8	Tubercidin	H	C	4.55±0.26	28
3	9	Toyocamycin	N≡	C	4.04±0.01	90
4	10	Sangivamycin	H ₂ N-C=O	C	5.49±0.02	3.3

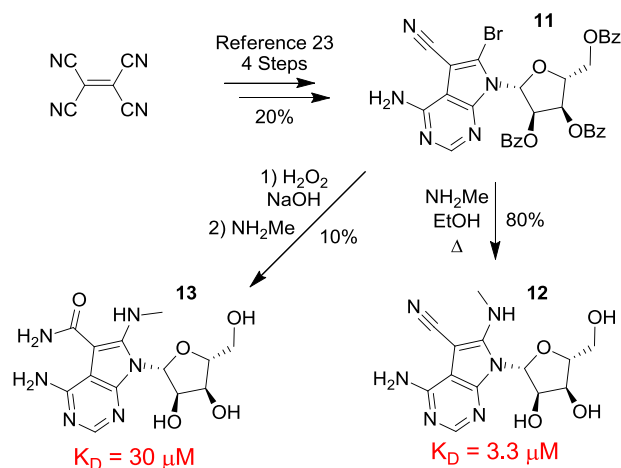
^aAll compounds were purchased from the relevant commercial suppliers and used without further purification. ^bAll results are quoted as the geometric mean±SEM of 3 independent experiments unless otherwise stated, pK_D=-log₁₀(K_D(μM)*10⁻⁶). ^cAll values are quoted to 2 significant figures.

We screened three commercially available bacterial natural products, all based on the replacement of the purine of adenosine with a pyrrolopyrimidine scaffold, exchanging the nitrogen at the 7-position with carbon.²² Comparing this change in scaffold to adenosine **1** (entry 1): the more lipophilic derivative tubercidin **8** (entry 2) displayed a 4-fold improvement in

affinity, substitution at the 7-position was well tolerated, with the nitrile derivative toyocamycin **9** (entry 3) displaying comparable affinity, and the primary amide derivative sangivamycin **10** (entry 4) gave a 35-fold increase in affinity at 3.3 μM .

With knowledge of the increased affinity observed with the pyrrolopyrimidine scaffold in hand, we planned to combine the scaffold hop with the improved affinity previously described for 8-amino substitution of the adenosine scaffold. 8-Amino substitution of tubercidin proved synthetically intractable due to the absence of an electron-withdrawing group at the 7-position making aromatic substitution at the 8-position challenging. Therefore, we focused our efforts on the synthesis of 8-aminotoyocamycin **12** and 8-aminosangivamycin **13** (Scheme 1).

Scheme 1. Natural product derived ligands of HSP70

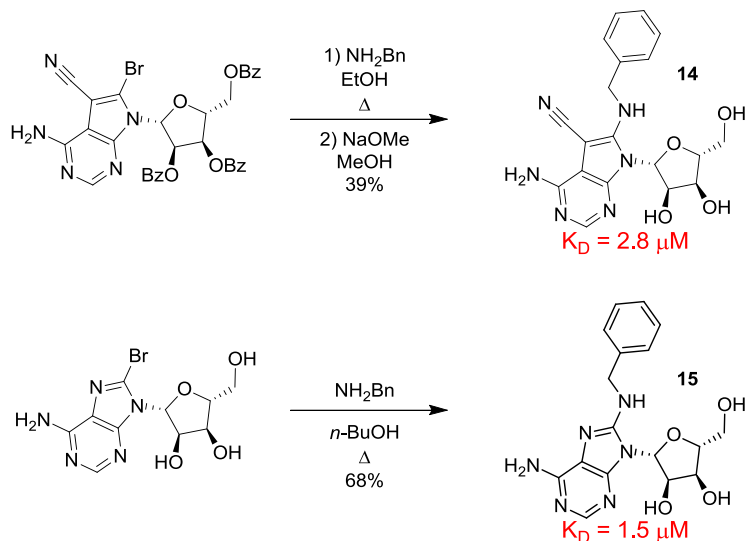


Tribenzoyl intermediate **11** was prepared in four steps and 20% yield using a previously described procedure.²³ Despite repeated attempts, we were unable to introduce an ammonia equivalent to the 8-position. However, we were successful using methylamine as a nucleophile to give 8-*N*-methylaminotoyocamycin **12**, which underwent *in situ* deprotection of the benzoyl groups under the reaction conditions. Treatment of intermediate **11** with basic hydrogen peroxide resulted in hydrolysis of the nitrile group and subsequent addition of methylamine gave 8-*N*-

methylaminosangivamycin **13** in low yield and moderate purity.²⁴ 8-*N*-Methylaminotoyocamycin **12** gave a $pK_D = 5.47 \pm 0.02$ ($K_D = 3.3 \mu\text{M}$, $n = 3$) against tr-HSC70. This result represented a 27-fold improvement in activity compared to toyocamycin **9** (Table 2, entry 1) and a 5-fold increase in affinity when compared to the corresponding 8-*N*-methyladenosine **12** (Table 1, entry 2). In contrast, 8-*N*-methylsangivamycin **13** gave a $pK_D = 4.52$ ($K_D = 30 \mu\text{M}$, $n = 1$),²⁵ which is a 7-fold drop in affinity compared to sangivamycin **10** (Table 2 entry 3). We rationalized this SAR through the potential effect of the 7-substituent on the hydrogen bonding ability of the key 8-*N*-methylamino group. The 7-position primary amide substituent of **13** can form an intramolecular hydrogen bond with the 8-*N*-methylamino group to give a resonance stabilized 6-membered intramolecular hydrogen bond,²⁶ which would mask the hydrogen bond donor effect of the 8-*N*-methylamino substituent and block the binding of this ligand.

In order to develop the toyocamycin scaffold further, we sought to introduce a benzylic substituent to the 8-position amine. Previously, Massey *et al.* have shown that *N*-benzyl substitution at the 8-amino position could improve the affinity of adenosine derived inhibitors of HSP70 (Figure 1).⁷ Since our toyocamycin derived scaffold **12** had displayed a 5-fold improvement in affinity compared to the corresponding adenosine scaffold **4**, we hypothesized that addition of an 8-*N*-benzyl substituent to toyocamycin would result in an improved chemotype for HSP70 inhibition. 8-*N*-Benzyltoyocamycin **14** was prepared *via* a similar method to **12**, using benzylamine as a nucleophile and subsequent deprotection of benzoyl protecting groups using sodium methoxide. For comparison 8-*N*-Benzyladenosine **15** was prepared in one-step *via* a literature procedure from commercially available 8-bromoadenosine (Scheme 2).²⁷

Scheme 2. 8-*N*-Benzyl derivatives of adenosine analogues



8-*N*-Benzyladenosine derivative **15** gave a $\text{pK}_D = 5.84 \pm 0.02$ ($K_D = 1.5 \mu\text{M}$, $n = 3$) representing a 12-fold improvement in binding affinity compared to the 8-*N*-methyladenosine analogue **4** (Table 1, entry 2); however, the 8-*N*-benzyltoyocamycin analogue **14** gave a $\text{pK}_D = 5.56 \pm 0.02$ ($K_D = 2.8 \mu\text{M}$, $n=3$), representing little change in affinity compared to 8-*N*-methyltoyocamycin derivative **12**, despite the increase in molecular weight. Even though toyocamycin **9** was apparently an improved scaffold, when compared to adenosine for the inhibition of HSP70, we had been unable to develop the compounds beyond a micromolar affinity ligand. We believed that improving our understanding of the complex SAR surrounding the nucleoside core and lipophilic 8-*N*-benzyl substituent would be crucial to the discovery and development of small-molecule inhibitors of HSP70.

HSP70 CONFORMATIONS

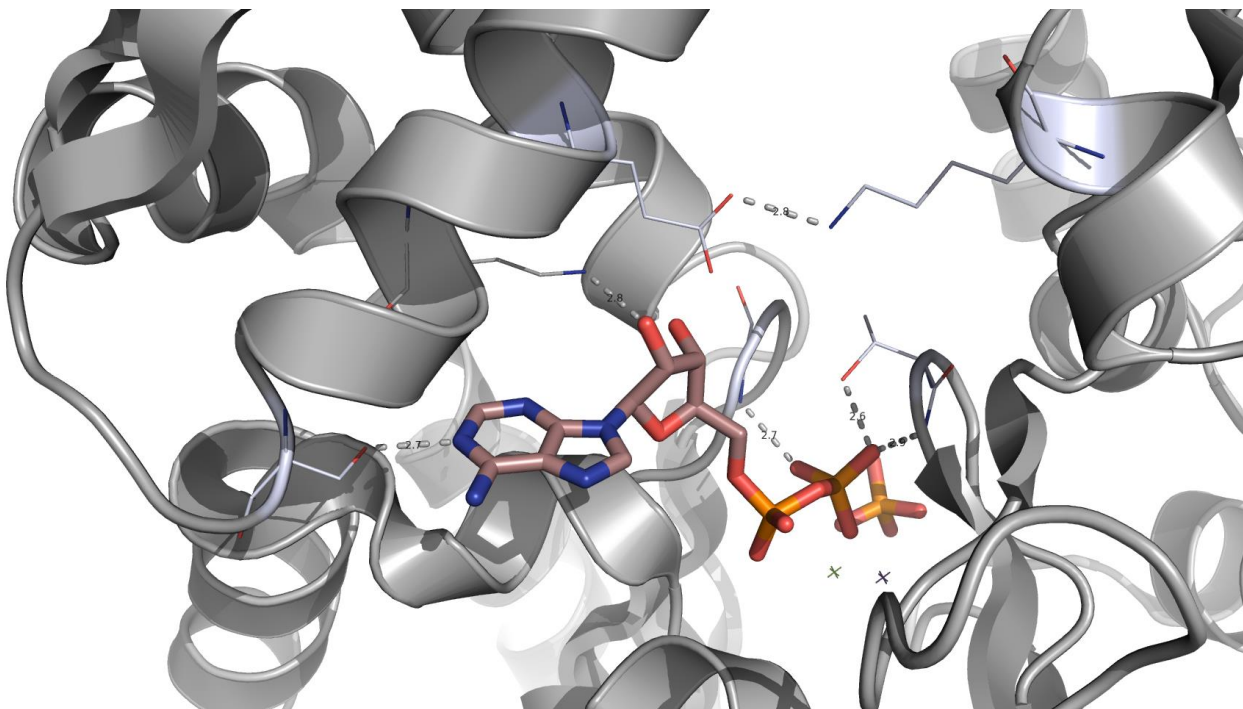
The biochemical mechanisms of the refolding activity of HSP70 have been the subject of numerous publications.¹⁴ In 1995, kinetic studies by McKay and Ha using changes in tryptophan fluorescence indicated that the HSP70 isoform, HSC70, undergoes a number of conformational changes in the catalytic cycle.²⁸ The energy released from ATP hydrolysis drives subsequent

conformational changes in the substrate binding domain, allowing HSP70 to carry out its refolding function on client proteins. However, what McKay and Ha discovered was that ATP and ADP have two distinct binding mechanisms. Whilst ADP binds and dissociates in a single-step, the binding of ATP is a two-step process, requiring a conformational change of the nucleotide binding domain prior to ATP hydrolysis. We hypothesized that the complexity surrounding the apparent SAR of the nucleoside derived HSP70 inhibitors was due to a flip in mechanism between a one-step and an induced conformational change two-step mechanism.²⁹

In order to investigate whether a two-step binding model is consistent with the observed nucleoside SAR, we decided to utilize the X-ray crystallography of the HSP70/ligand complex. There is currently no full-length crystal structure of human HSP70 and we were also unsuccessful in our attempts to generate such a structure. We therefore focused our crystallography efforts on the nucleotide binding domain (NBD) of the human HSP70 isoform HSP72. Since we wanted to investigate ligand induced conformational changes of HSP70 a ligand soaking strategy would be inappropriate, as the crystal would either limit conformational change or block the binding of ligands. We therefore developed a small molecule/protein co-crystallization protocol, which would allow us to observe a greater range of ligand-bound protein conformations.³⁰

In our hands, ADP **16** gave an affinity of $pK_D = 6.49$ ($K_D = 0.32 \mu\text{M}$, $n = 1$) when measured by SPR against the tr-HSC70.³¹ The co-crystal structure of ADP/ P_i bound to the nucleotide binding domain of HSP72 clearly revealed a closed conformation of the protein. The two α -helices closed around the adenosine motif of ADP, forming multiple hydrogen bonds with the ribose and adenine fragments (Figure 3).

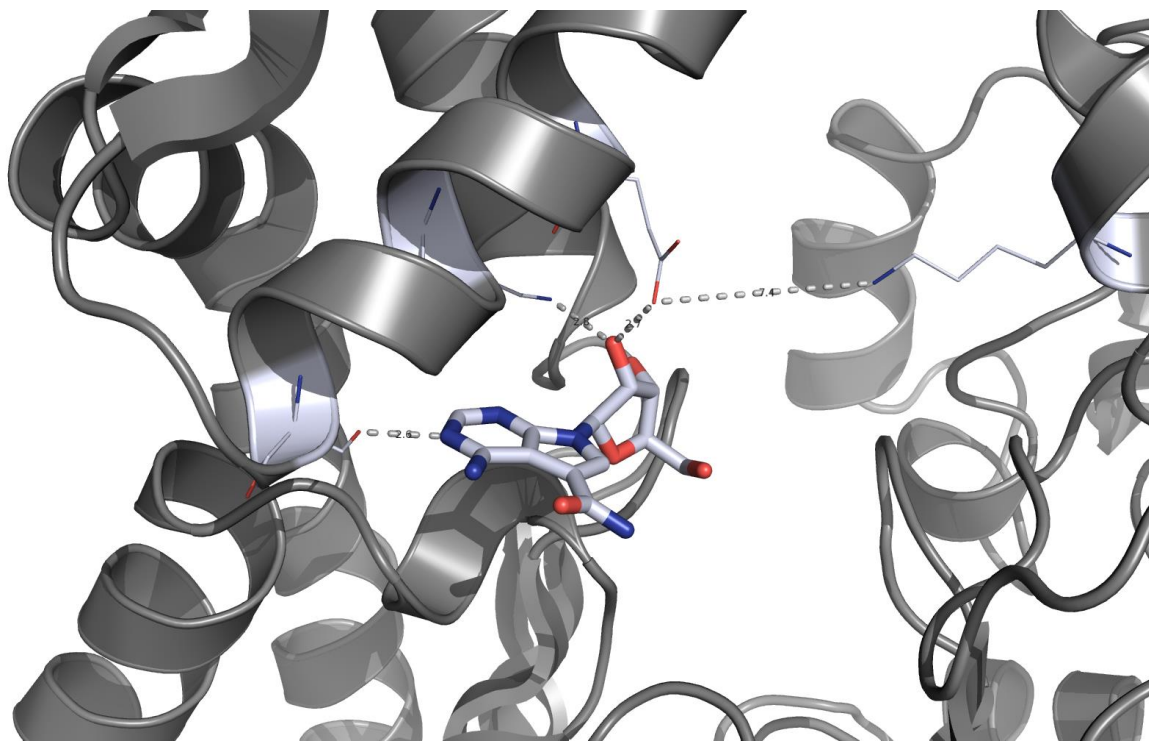
Figure 3. Crystal Structure of ADP/ P_i bound to HSP72



PDB: 3ATU, key hydrogen bonding interactions and their distances in Angstroms are indicated. The key salt-bridge interaction between lysine-56 and glutamic acid-268 was measured at 2.9 Å. Purple and green stars represent sodium and magnesium ions respectively.

In the structure, the two phosphate groups of ADP form multiple hydrogen bonds within the phosphate binding region of tr-HSP72. It is clear from this structure that tr-HSP72 would need to undergo a conformational change in order for ADP/P_i to dissociate. An interesting observation from the analysis of this structure was that in order to observe the closed conformation, with the protein enveloping the ligand, it is necessary for the two α-helices to come in close proximity to each other. The ligand/protein co-crystal structure, rather than a structure obtained by soaking reveals this conformation is apparently stabilized by the formation of a solvent exposed salt-bridge between glutamic acid-268 and lysine-56.³² Intrigued by this apparent formation of this novel intramolecular interaction, we then sought to generate a co-crystal structure of the bacterial natural product sangivamycin **10** ($K_D = 3.3 \mu\text{M}$) (Figure 3).

Figure 3. Co-crystal structure of Sangivamycin **10** bound to HSP72

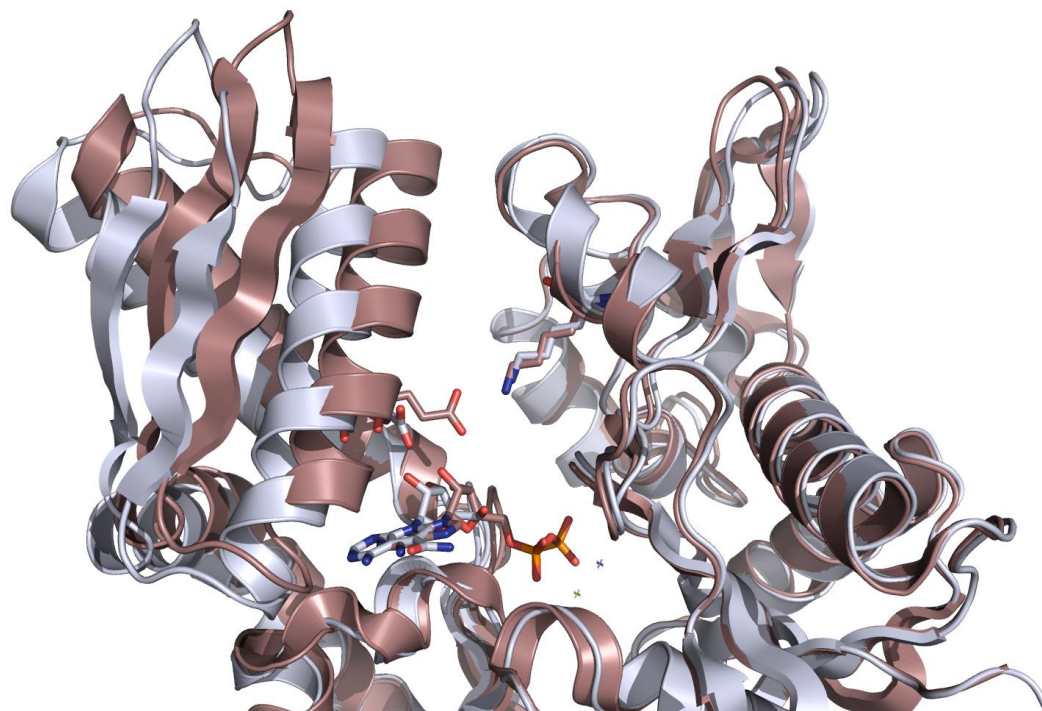


Key hydrogen bonding interactions and their distances in Angstroms are indicated. The key salt-bridge interaction between lysine-56 and glutamic acid-268 was measured at 7.4 Å.

The crystal structure of sangivamycin **10** revealed a similar hydrogen bonding framework to the adenosine motif of the ADP/P_i structure (Figure 3). The pyrrolopyrimidine ring interacts with serine-275 and the 2'- and 3'-hydroxyls of the ribose interacts with lysine-271. However, in contrast to ADP/P_i, sangivamycin **10** co-crystallized in an open conformation of tr-HSP72; whereby, the two α -helices of the nucleotide binding domain are no longer in close proximity, so no solvent exposed salt-bridge is able to form between glutamic acid-268 and lysine-56. It is this difference in the binding conformation which we hypothesize is an important factor in the complexity of SAR observed with nucleoside derived inhibitors of HSP70. The binding of both ADP/P_i **16** and sangivamycin **10** are dominated by the formation of multiple hydrogen bonds to key residues in the nucleoside binding cleft but the key difference between the two ligands is their ability to induce and stabilize the closed conformation of tr-HSP72. It is this ligand-driven induced conformational change that leads to high affinity inhibitors of HSP70. The conformation

change observed with ADP/P_i **16** is presumably brought about by the interactions of the β -phosphate group of ADP with the glycine rich loops of the phosphate binding region. This conformational change could force water molecules from the nucleotide binding domain cleft, strengthening the many hydrogen bond contacts surrounding the adenosine ring and especially the ribose ring, due to the more hydrophobic environment. The absence of a β -phosphate group in sangivamycin **10** means there is no induced conformational change so affinity is only dependent on the multiple hydrogen bonds (Figure 4).

Figure 4. Induced open and induced closed conformations of HSP72

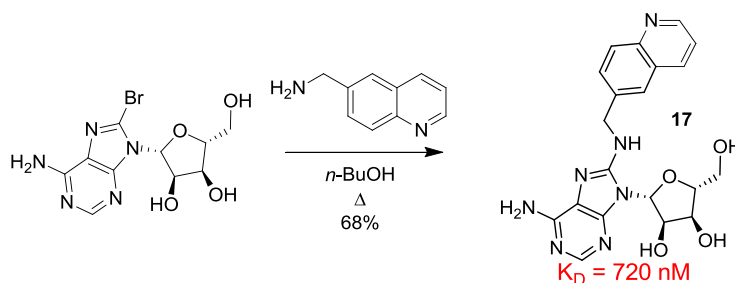


The copper structure describes the co-crystal structure of ADP/P_i bound to HSP72 in the induced closed conformation, due to interactions of the phosphate groups through hydrogen bonds with the glycine rich loops and stabilized by the salt-bridge. The grey structure describes the co-crystal structure of Sangivamycin **10** bound to HSP72. The overlay clearly shows Sangivamycin **10** crystallizes in the open conformation, such that formation of the key salt bridge is not possible.

MIMICKING THE β -PHOSPHATE

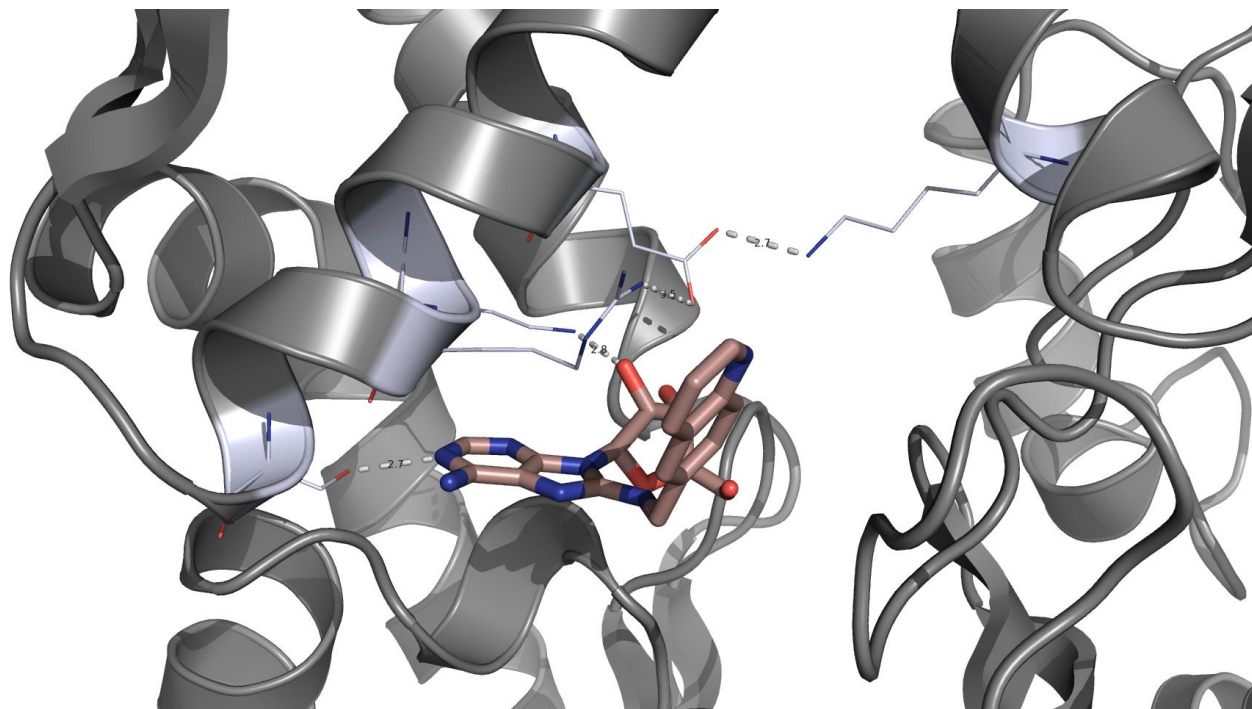
Mimicking phosphate groups with druglike ligands represents a significant challenge in medicinal chemistry.³³ However, if it is possible to induce the closed conformation of the HSP70 nucleotide binding domain *via* an alternative mechanism, then mimicking the β -phosphate of ADP would be unnecessary. Since the only new enthalpic intra-protein interaction that we could observe in the closed tr-HSP72 structure, when compared with the open sangivamycin **10** structure, was the solvent exposed salt-bridge between glutamic acid-268 and lysine-56, we hypothesized that any ligand stabilizing this interaction would stabilize the closed conformation of HSP70, leading to increased affinity. We therefore proposed that the previously described potent 8-*N*-benzyladenosine derived ligands were able induce a conformational change in the HSP70 but *via* a more lipophilic mechanism, which would be more amenable to drug discovery. In order to investigate this hypothesis we synthesized the known quinoline derived HSP70 inhibitor **17**, in one step and 68% yield using our previously described method (Scheme 3).⁷

Scheme 3. Synthesis of quinoline adenosine derivative



Although several 8-*N*-substituted HSP70 inhibitors have been described in the literature,⁷ the 8-*N*-quinoline adenosine derived ligand **17** was chosen since it was reported to be the highest affinity ligand which was only substituted at the 8-position. In our hands, **17** gave a $\text{p}K_D = 6.14 \pm 0.01$ ($K_D = 0.72 \text{ } \mu\text{M}$, $n = 3$) against tr-HSC70 when measured by SPR, which was consistent with the data reported in the literature.³⁴ 8-*N*-Quinoline aminoadenosine derived ligand **17** was then submitted to our co-crystallization protocol with tr-HSP72 (Figure 5).

Figure 5. Co-crystallization of 8-*N*-Quinoline aminoadenosine derived ligand **17** bound to HSP72



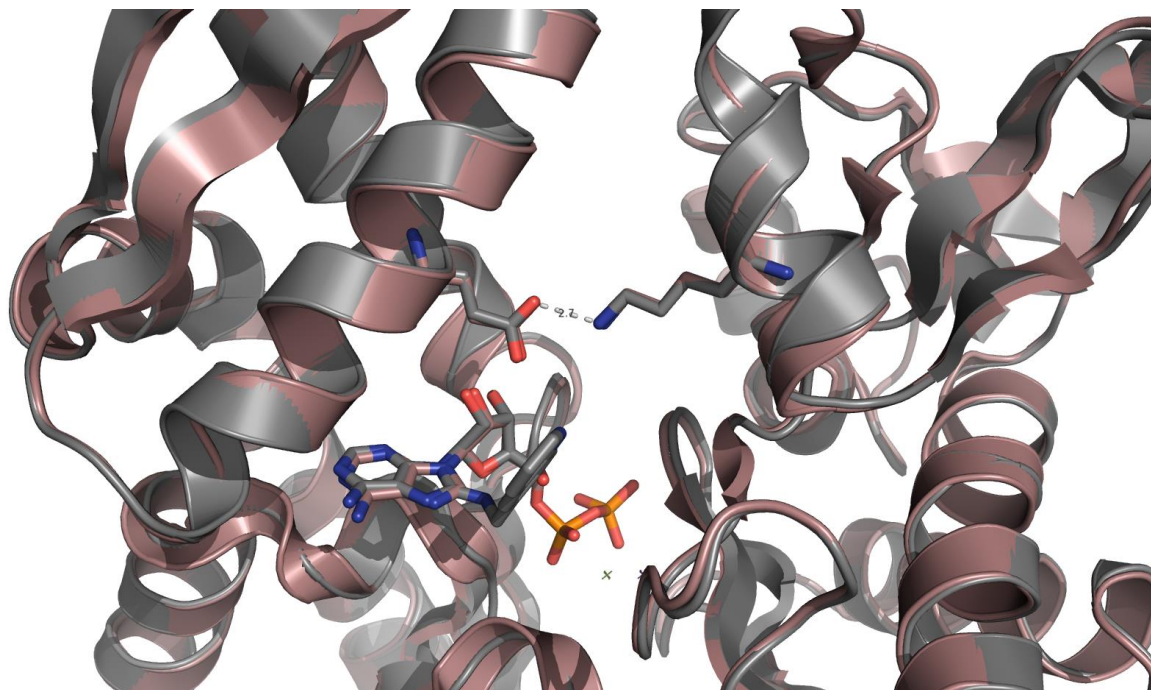
The grey structure clearly demonstrates the formation the key salt-bridge when co-crystallized with 8-*N*-quinolineadenosine **17**. Important hydrogen bonding interactions are indicated with their distances in Angstroms.

When **17** was co-crystallized with the nucleotide binding domain of HSP72 we found that the protein had crystallized in its closed conformation. The conformation of tr-HSP72 induced by **17** was superimposable on the co-crystal structure of ADP/P_i with tr-HSP72 (Figure 6). To our knowledge, this is the first example of a co-crystal structure demonstrating a non-nucleotide ligand binding to the closed conformation of HSP70. The similarity between the HSP70 conformation observed with ADP/P_i and 8-*N*-quinoline adenosine **15** co-crystal structures is consistent with the potential importance of the induced conformational change to the affinity of the 8-*N*-benyl nucleoside derived inhibitors of HSP70. However, the mechanism by which the

induced conformational change occurs must be distinctly different, since the quinoline moiety of **17** forms no interactions within the phosphate binding region.

In order to rationalize the induced conformational change observed with **17** we further analyzed the closed structure of tr-HSP72 to identify the key binding interactions. 8-*N*-Quinoline adenosine **17** displays a similar hydrogen bonding network with the same key residues observed in both ADP/P_i and sangivamycin **10**. However, in contrast with the open conformation observed with sangivamycin **10**, the closed conformation of tr-HSP72 and quinoline **27** clearly showed the key salt-bridge interaction between glutamic acid-268 and lysine-56 binding the two α -helices of the nucleotide binding cleft, the same salt-bridge predicted from the ADP/P_i structure (Figure 5). In the ADP/P_i/tr-HSP72 co-crystal structure the salt-bridge is solvent exposed, weakening its effect.³⁵ By contrast, in the **17**/tr-HSP72 co-crystal structure the quinoline moiety is able π -stack against arginine-272. Although this interaction is solvent exposed so is only likely to be weak,³⁶ the result is to place the quinoline group directly in front of the salt-bridge. Since the quinoline is highly lipophilic, this creates a more lipophilic environment surrounding the salt-bridge, protecting it from water and strengthening the interaction, which leads to increased affinity for 8-*N*-benzyl aminonucleoside derived ligands.³⁷ We propose the binding mechanism of such ligands to HSP70 is analogous to a “door and latch”. The initial binding event is similar for all nucleoside derived ligands of HSP70 and is dominated by hydrogen bonds to serine-275 and lysine-271. The nucleotide binding domain is then able to close around the ligand; however, for this process to be favorable it must be stabilized by the ligand. ADP can achieve this through interactions with the phosphate binding region, whilst quinoline ligand **17** stabilizes the key salt-bridge through hydrophobic desolvation. Sangivamycin **10** has neither of these substituents so predominately binds to the open conformation.

Figure 6. Overlay of ADP/P_i and 8-*N*-Quinoline adenosine **17** co-crystal structures with HSP72

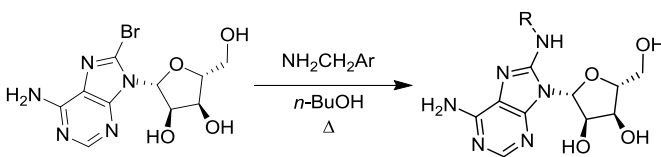


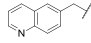
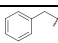
Overlay of the ADP/P_i-HSP72 co-crystal structure (grey) and the 8-*N*-Quinolineadenosine **17**-HSP72 co-crystal structure (copper). The key salt-bridge is highlighted with a distance of 2.7 Å.

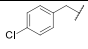
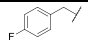
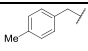
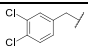
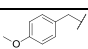
OPTIMIZING THE 8-POSITION

In order to test this hypothesis, and to generate more active ligands of HSP70 for further development, we synthesized a series of 8-*N*-benzylaminoadenosine analogues using the previously described method.

Table 3. The 8-position optimization of adenosine derived HSP70 ligands



Entry	Compd.	R	pK _D ±SEM ^a	K _D (μM) ^b
1	17		6.14±0.01	0.72
2	15		5.84±0.02	1.4

3	18		6.55±0.01 ^c	0.28
4	19		6.34±0.01	0.46
5	20		6.53±0.01	0.30
6	21		5.45±0.01	3.5
7	22		5.73±0.01	1.9

^aAll results are quoted as the geometric mean±SEM of 3 independent experiments unless otherwise stated, $pK_D = -\log_{10}(K_D(\mu M) * 10^{-6})$. ^bAll values are quoted to 2 significant figures. ^cThe geometric mean of n=9 experiments.

The 8-*N*-benzyl derivative **15**, as shown previously, gave a $pK_D = 5.84 \pm 0.02$ ($K_D = 1.4 \mu M$, n=3) when measured by SPR against tr-HSC70. The weaker activity observed with the benzyl group **15** compared to quinoline **17** we rationalized is due to its less efficient desolvation of the glutamic acid/lysine salt bridge by the smaller lipophilic group. Therefore, we decided to add a number of lipophilic substituents to assess whether we could improve the desolvation effect, promote the induced closed conformation and improve the affinity of the ligands. *para*-Chloro-substitution to give adenosine derivative **18** (Entry 3) gave a $pK_D = 6.55 \pm 0.01$ ($K_D = 0.28 \mu M$, n = 9), a 5-fold improvement in affinity compared to compound **15** and a 60-fold improvement compared to 8-*N*-methylaminoadenosine. Similar improvements were also observed for the *para*-fluoro **19** (Entry 4, $pK_D = 6.34 \pm 0.01$, $K_D = 0.46 \mu M$, n=3) and *para*-methyl (Entry 5, $pK_D = 6.53 \pm 0.01$, $K_D = 0.30 \mu M$, n=3). Since the crystal structures of this ligand class show that the benzylic moiety resides in the cleft formed by the two α -helices in the nucleotide binding domain of HSP70, it is unlikely that the *para*-lipophilic substituents interact with HSP70 *via* a lipophilic pocket, as the group is essentially solvent exposed. This effect could not be explained by an increase in the overall lipophilicity of the ligand to exploit the non-specific hydrophobic effect, since dichlorobenzyl derivative **21** (Entry 6, $pK_D = 5.45 \pm 0.01$, $K_D = 3.5 \mu M$, n =3)

displayed a significant drop in affinity. The effect of desolvation was highlighted for the *para*-methoxy analogue **22** (Entry 7, $pK_D = 5.73 \pm 0.01$, $K_D = 1.9 \mu\text{M}$, $n = 3$), which can be explained by a steric clash with the salt-bridge in the induced closed conformation destabilizing the interaction and resulting in a lower affinity ligand.

CONCLUSIONS

HSP70 is a challenging protein to target with small molecules due to the hydrophilic nature of the nucleotide binding site and the high flexibility of that binding site. In order to target the nucleotide binding domain it is important to understand the conformational changes that this region of the protein undergoes. Using protein/ligand X-ray crystallography, we have demonstrated for the first time that non-nucleotide ligands of HSP70 can induce conformational changes in the protein and that these changes can play an important role in the binding of HSP70 inhibitors. The use of X-ray crystallography in the study of HSP70 conformations and their importance in inhibitor design remains in its early stages. In solution, kinetic studies suggest that this protein undergoes a number of conformational changes of not just the nucleotide binding domain but also the substrate binding domain.²⁸ Also, interactions between these two domains and the role of co-chaperones in these conformational changes have yet to be addressed. Better understanding of the flexibility of HSP70 and its effect on the affinity of ligands will contribute to better assay design and more efficient inhibitor optimization and in the future.

AUTHOR INFORMATION

Corresponding Author

*Author to whom correspondence should be addressed.

Author Contributions

The manuscript was written through contributions of all authors. All authors have given approval to the final version of the manuscript. ‡These authors contributed equally. (match statement to author names with a symbol)

EXPERIMENTAL SECTION

Supporting Information Available: Experimental procedures for all compounds and intermediates, copies of ¹H-NMR and ¹³C-NMR of final compounds, details of commercially available analogues, supporting SPR data and sensorgrams, complete SPR methods and crystallography details. This material is available free of charge via the Internet at <http://pubs.acs.org>.

Experimental Procedures (Chemistry)

Unless otherwise stated, reactions were conducted in oven dried glassware under an atmosphere of nitrogen using anhydrous solvents. All commercially obtained reagents and solvents were used as received. Thin layer chromatography (TLC) was performed on pre-coated aluminum sheets of silica (60 F254 nm, Merck) and visualized using short-wave UV light. Flash column chromatography was carried out on Merck silica gel 60 (particle size 40-65 μm). ¹H NMR spectra were recorded on Bruker AMX500 (500 MHz) spectrometers using an internal deuterium lock. Chemical shifts are quoted in parts per million (ppm) using the following internal references: CDCl₃ (δ_H 7.26), MeOD (δ_H 3.31) and DMSO-d₆ (δ_H 2.50). Signal splitting are recorded as singlet (s), doublet (d), triplet (t), quartet (q) and multiplet (m), doublet of doublets (dd), doublet of doublet of doublets (ddd), apparent triplet (app. t) and broad (br.). Coupling constants, *J*, are measured to the nearest 0.1 Hz. ¹³C-NMR spectra was recorded on Bruker AMX500 spectrometers at 126 MHz using an internal deuterium lock. Chemical shifts are quoted to 0.01 ppm, unless greater accuracy was required, using the following internal references: CDCl₃ (δ_C

77.0), MeOD (δ C 49.0) and DMSO-d₆ (δ C 39.5). High resolution mass spectra were recorded on an Agilent 1200 series HPLC and diode array detector coupled to a 6210 time of flight mass spectrometer with dual multimode APCI/ESI source. Analytical separation was carried out on a Merck Purospher STAR RP-18, 30x4 mm column using a flow rate of 1.5 mL/min in a 4 minute gradient elution, UV detection was at 254 nm. All compounds were >95% purity by HPLC analysis unless otherwise stated.

(2R,3R,4S,5R)-2-(6-amino-8-(methylamino)-9H-purin-9-yl)-5-(hydroxymethyl)tetrahydrofuran-3,4-diol 4

To a solution of 8-bromoadenosine (0.051 g, 0.147 mmol) in EtOH (1.473 ml) was added methylamine solution (33% solution in EtOH, 0.247 ml, 2.95 mmol) and the mixture was heated to 80 °C for ~12 hrs. After this time the mixture was cooled to room temperature and the solvent removed under reduced pressure. The resulting residue was purified by silica gel chromatography eluting with 2 M MeOH/NH₃:EtOAc (8:2) to give the desired compound as a white solid (0.031 g 71%); δ H (500 MHz, DMSO-d₆) 7.90 (s, 1H), 6.95 (d, J = 4.8 Hz, 1H), 6.57 (s, 2H), 5.92 (dd, J = 6.0, 4.0 Hz, 1H), 5.86 (d, J = 7.3 Hz, 1H), 5.26 (d, J = 6.7 Hz, 1H), 5.16 (d, J = 4.0 Hz, 1H), 4.68 (td, J = 7.0, 5.3 Hz, 1H), 4.12 (ddd, J = 5.6, 4.1, 2.1 Hz, 1H), 3.97 (d, J = 2.3 Hz, 1H), 3.70 - 3.58 (m, 2H), 2.89 (d, J = 4.5 Hz, 3H); δ C (126 MHz, DMSO-d₆) 152.86, 152.52, 150.28, 148.89, 117.64, 86.99, 86.13, 71.42, 71.20, 62.15, 29.59; HRMS (ESI) C₁₁H₁₇N₆O₄ (M+H⁺) requires 297.1306, found 297.1299.

(2R,3R,4S,5R)-2-(6-amino-8-(dimethylamino)-9H-purin-9-yl)-5-(hydroxymethyl)tetrahydrofuran-3,4-diol 5

To a solution of 8-bromoadenosine (0.064 g, 0.185 mmol) in EtOH (1.849 ml) was added dimethylamine (40% solution in water, 0.416 ml, 3.70 mmol) and the mixture was heated to 80

°C for ~12 hrs. After this time the mixture was cooled to room temperature and the solvent removed under reduced pressure. The resulting residue was purified by silica gel chromatography eluting with 2 M MeOH/NH₃:EtOAc (9:1) to give the desired product as a white solid (0.027 g, 47%); δ H (500 MHz, MeOH) 8.05 (d, J = 1.1 Hz, 1H), 5.91 (d, J = 7.5 Hz, 1H), 5.16 (dd, J = 7.5, 5.3 Hz, 1H), 4.36 (dd, J = 5.2, 1.4 Hz, 1H), 4.14 (d, J = 1.9 Hz, 1H), 3.86 (dd, J = 12.6, 2.3 Hz, 1H), 3.73 (dd, J = 12.6, 2.7 Hz, 1H), 3.03 (s, 6H); δ C (126 MHz, MeOD). 157.19, 153.92, 149.92, 149.22, 116.86, 89.06, 86.97, 71.96, 71.79, 62.86, 41.89; HRMS (ESI) C₁₂H₁₉N₆O₄ (M+H⁺) requires 311.1462, found 311.1464.

(2R,3R,4S,5R)-2-(6-amino-8-methoxy-9H-purin-9-yl)-5-(hydroxymethyl)tetrahydrofuran-3,4-diol

6

(2R,3R,4S,5R)-2-(6-amino-8-(methylamino)-9H-purin-9-yl)-5-methyltetrahydrofuran-3,4-diol **7**

To a solution of 5'-deoxyadenosine (0.024 g, 0.096 mmol) in dioxane (0.478 ml) and water (0.478 ml) was added KHPO₄ (0.065 g, 0.287 mmol) and bromine (0.023 g, 0.143 mmol) as a solution in water (0.5 ml) and the mixture was stirred for 15 minutes. The mixture was then quenched sat. sodium thiosulfate solution (5 ml), extracted with EtOAc, dried (MgSO₄) and the solvent removed under reduced pressure. The resulting residue was used in the next step without further purification.

The product from the previous step (0.032 g, 0.097 mmol) was dissolved in 2 M MeNH₂ in EtOH (1.939 ml) and the mixture was heated to 70 °C for ~12 hrs. After this time the mixture was cooled to room temperature and the solvent removed under reduced pressure. The resulting residue was purified by silica gel chromatography eluting with 2 M MeOH/NH₃:EtOAc (1:9) to give the desired product as a white solid (0.009 g, 33% over two steps); δ H (500 MHz, DMSO-

d6) 7.90 (s, 1H), 6.75 (q, $J = 4.5$ Hz, 1H), 6.45 (s, 2H), 5.58 (d, $J = 4.2$ Hz, 1H), 5.23 (d, $J = 5.0$ Hz, 1H), 5.09 (q, $J = 5.0$ Hz, 1H), 4.99 (d, $J = 5.7$ Hz, 1H), 4.14 - 4.04 (m, 1H), 3.83 (app. p, $J = 6.2$ Hz, 1H), 2.88 (d, $J = 4.5$ Hz, 3H), 1.24 (d, $J = 6.3$ Hz, 3H); δ C (126 MHz, DMSO-d6) 152.97, 152.91, 150.19, 149.12, 117.95, 88.07, 79.10, 74.87, 71.05, 29.73, 18.96; HRMS (ESI) $C_{11}H_{17}N_6O_3$ ($M+H^+$) requires 281.1357, found 281.1354.

(2R,3R,4R,5R)-2-(4-amino-6-bromo-5-cyano-7H-pyrrolo[2,3-d]pyrimidin-7-yl)-5-((benzoyloxy)methyl)tetrahydrofuran-3,4-diyl dibenzoate 11

Prepared via a previously described procedure in 4 steps and 20% overall yield. The spectroscopic data matched that previously described.³⁸

4-amino-7-((2R,3R,4S,5R)-3,4-dihydroxy-5-(hydroxymethyl)tetrahydrofuran-2-yl)-6-(methylamino)-7H-pyrrolo[2,3-d]pyrimidine-5-carbonitrile 12

(2R,3R,4R,5R)-2-(4-amino-6-bromo-5-cyano-7H-pyrrolo[2,3-d]pyrimidin-7-yl)-5-

((benzoyloxy)methyl)tetrahydrofuran-3,4-diyl dibenzoate 11 (118 mg, 0.174 mmol) was dissolved in 2 M methylamine in ethanol(5 ml) and the reaction was heated in a microwave reactor at 140 °C for 1 hr. After this time, the mixture was cooled to room temperature and the solvent removed under reduced pressure. The resulting residue was purified by silica gel chromatography with the Biotage SP1 purification system (column: 10+S; flow rate, 15ml/min; gradient starting with 100% DCM from 0 to 1 CV then from 100% DCM to 2% $NH_4OH/18\%$ MeOH/80% DCM from 1 CV to 21 CV) to give the desired compound as a white solid (0.045 g, 80% yield); δ H (500 MHz, MeOD) 3.22 (s, 3H), 3.83-3.84 (m, 2H), 4.14 (q, $J = 1.9$ Hz, 1H), 4.27 (dd, $J = 5.6, 2.0$ Hz, 1H), 4.65 (dd, $J = 7.6, 5.6$ Hz, 1H), 6.29 (d, $J = 7.9$ Hz, 1H), 8.01 (s, 1H); δ C (126 MHz, MeOD) 29.55, 61.31, 70.91, 71.19, 86.12, 87.35, 101.19, 118.75, 148.27, 149.87, 151.26, 154.16; HRMS (ESI) $C_{13}H_{17}N_6O_4$ ($M+H^+$) requires 321.1306, found 321.1303.

4-amino-7-((2R,3R,4S,5R)-3,4-dihydroxy-5-(hydroxymethyl)tetrahydrofuran-2-yl)-6-(methylamino)-7H-pyrrolo[2,3-d]pyrimidine-5-carboxamide 13

To a solution of (2R,3R,4R,5R)-2-(4-amino-6-bromo-5-cyano-7H-pyrrolo[2,3-d]pyrimidin-7-yl)-5-((benzyloxy)methyl)tetrahydrofuran-3,4-diyl dibenzoate **11** (87 mg, 0.127 mmol) in THF (1 mL), was added hydrogen peroxide (33%, 1 ml) and 1 M NaOH (1 ml). The reaction was stirred at room temperature for ~18 hrs before 1 M HCl was added until the mixture reached pH 6 when the solvent was removed under reduced pressure. The resulting residue was dissolved in 2 M methylamine in ethanol (5 ml) and the reaction was heated to 120 °C in a microwave reactor for 50 min. After this time the mixture was cooled to room temperature and the solvent removed under reduced pressure. The resulting residue was purified by silica gel chromatography using the Biotage SP1 purification system (Column: 10+S; Flow rate, 15ml/min; gradient starting with 100% DCM from 0 to 1 CV then from 100% DCM to 2% NH₄OH/18% MeOH/80% DCM from 1 CV to 21 CV) to give the desired product as a yellow solid (0.009 g, 10% yield); δ H (500 MHz, MeOD) 2.89 (s, 3H), 3.78 (dd, $J = 12.2, 1.9$ Hz, 1H), 3.86 (dd, $J = 12.2, 2.2$ Hz, 1H), 4.18 (q, $J = 1.7$ Hz, 1H), 4.33 (dd, $J = 5.5, 1.3$ Hz, 1H), 4.85 (m, 1H), 6.12 (d, $J = 7.9$ Hz, 1H), 8.02 (s, 1H); δ C (126 MHz, MeOD) 35.35, 62.23, 71.62, 72.28, 86.70, 87.49, 98.51, 101.02, 146.72, 147.31, 150.61, 157.30, 167.61; HRMS (ESI) C₁₃H₁₉N₆O₅ (M+H⁺) requires 339.1411, found 339.1408.

4-amino-6-(benzylamino)-7-((2R,3R,4S,5R)-3,4-dihydroxy-5-(hydroxymethyl)tetrahydrofuran-2-yl)-7H-pyrrolo[2,3-d]pyrimidine-5-carbonitrile 14

(2R,3R,4R,5R)-2-(4-amino-6-bromo-5-cyano-7H-pyrrolo[2,3-d]pyrimidin-7-yl)-5-((benzyloxy)methyl)tetrahydrofuran-3,4-diyl dibenzoate **11** (31 mg, 0.045 mmol) was dissolved in EtOH (2 mL) and benzylamine (29 mg, 0.27 mmol) was added to the solution. The reaction

was heated in a microwave reactor at 160 °C for 1 hr. After this time the mixture was cooled to room temperature and the solvent removed under reduced pressure. The resulting residue was dissolved in methanol (0.5 ml) and 0.5 M sodium methoxide (1 mL) was added. The reaction was stirred at room temperature for 1 hr then the solvent was removed under reduced pressure. The resulting residue was purified by silica gel chromatography with the Biotage SP1 purification system (column: 10+S; flow rate, 15ml/min; gradient starting with 100% DCM from 0 to 1 CV then from 100% DCM to 2% NH₄OH/18% MeOH/80% DCM from 1 CV to 21 CV) to give the desired compound as a white solid (0.007 g, 39% yield); δ H (500 MHz, MeOD) 3.80-3.86 (m, 2H), 4.18 (q, J = 1.8 Hz, 1H), 4.28 (dd, J = 5.6, 1.7 Hz, 1H), 4.73 (dd, J = 7.8, 5.7 Hz, 1H), 4.78 (d, J = 10.3 Hz, 2H), 6.37 (d, J = 7.9 Hz, 1H), 7.25-7.27 (m, 1H), 7.33-7.36 (m, 2H), 7.41-7.43 (m, 2H), 8.01 (s, 1H); δ C (126 MHz, MeOD) 46.28, 61.40, 71.14, 71.29, 86.27, 87.38, 101.06, 118.30, 126.72, 126.98, 128.25, 138.41, 148.25, 149.94, 150.10, 154.22; HRMS (ESI) C₁₉H₂₁N₆O₄ (M+H⁺) requires 397.1619, found 397.1614.

(2R,3R,4S,5R)-2-(6-amino-8-(benzylamino)-9H-purin-9-yl)-5-(hydroxymethyl)tetrahydrofuran-3,4-diol 15

To a solution of 8-bromoadenosine (0.061 g, 0.176 mmol) in *n*-butanol (1.762 ml) was added ¹Pr₂NEt (0.092 ml, 0.529 mmol) and benzylamine (0.038 ml, 0.352 mmol) and the mixture was heated to 120 °C for ~16 hrs. After this time the mixture was cooled to room temperature and the resulting residue was purified by silica gel chromatography eluting with EtOAc:MeOH (95:5) to give the desired product as a white solid (0.017 g, 26%); δ H (500 MHz, MeOD) 8.00 (s, 1H), 7.45 - 7.38 (m, 2H), 7.37 - 7.32 (m, 2H), 7.28 - 7.23 (m, 1H), 6.11 (d, J = 7.7 Hz, 1H), 4.81 (dd, J = 7.6, 5.4 Hz, 1H), 4.69 (d, J = 15.8 Hz, 1H), 4.64 (d, J = 15.8 Hz, 1H), 4.30 (dd, J = 5.6, 1.6 Hz, 1H), 4.18 (q, J = 1.9 Hz, 1H), 3.85 (dd, J = 12.0, 2.3 Hz, 1H), 3.79 (dd, J = 11.9, 1.7 Hz,

1H); δ C (126 MHz, MeOD) 152.12, 151.99, 149.65, 148.63, 138.75, 128.11, 126.68, 126.52, 116.56, 87.29, 86.41, 71.64, 71.52, 61.75, 45.42; HRMS (ESI) $C_{17}H_{21}N_6O_4$ ($M+H^+$) requires 373.1619, found 373.1623.

(2R,3R,4S,5R)-2-(6-amino-8-((quinolin-6-ylmethyl)amino)-9H-purin-9-yl)-5-(hydroxymethyl)tetrahydrofuran-3,4-diol 17

To a solution of 8-bromoadenosine (0.099 g, 0.285 mmol) in *n*-butanol (2.85 ml) was added quinolin-6-ylmethanamine (0.045 g, 0.285 mmol) and iPr_2NEt (0.149 ml, 0.854 mmol) and the mixture was heated to 120 °C under N_2 for 24 hrs. After this time the mixture was cooled to room temperature and the solvent removed under reduced pressure. The resulting residue was purified by chromatography eluting with EtOAc:2 M MeOH/ NH_3 (80:20) to give the desired product as a white solid (0.008 g, 7%); δ H (500 MHz, MeOD) 8.83 (dd, $J = 4.4, 1.7$ Hz, 1H), 8.37 (dt, $J = 8.4, 1.2$ Hz, 1H), 8.04 (d, $J = 8.7$ Hz, 1H), 8.02 (s, 1H), 7.95 (d, $J = 1.8$ Hz, 1H), 7.86 (dd, $J = 8.8, 2.0$ Hz, 1H), 7.54 (dd, $J = 8.3, 4.3$ Hz, 1H), 6.16 (d, $J = 7.6$ Hz, 1H), 4.32 (dd, $J = 5.4, 1.7$ Hz, 1H), 4.21 (q, $J = 1.9$ Hz, 1H), 3.87 (dd, $J = 12.0, 2.3$ Hz, 1H), 3.80 (dd, $J = 11.9, 1.7$ Hz, 1H); δ C (126 MHz, MeOD) 151.98, 151.94, 149.72, 149.52, 148.44, 146.69, 137.89, 136.94, 129.30, 128.46, 127.90, 125.07, 121.35, 116.59, 87.38, 86.47, 71.70, 71.53, 61.75, 45.29; HRMS (ESI) $C_{20}H_{22}N_7O_4$ ($M+H^+$) requires 424.1728, found 424.1725.

(2R,3R,4S,5R)-2-(6-amino-8-((4-chlorobenzyl)amino)-9H-purin-9-yl)-5-(hydroxymethyl)tetrahydrofuran-3,4-diol 18

To a solution of 8-bromoadenosine (0.078 g, 0.225 mmol) in *n*-butanol (2.253 ml) was added iPr_2NEt (0.118 ml, 0.676 mmol) and (4-chlorophenyl)methanamine (0.055 ml, 0.451 mmol) and the mixture was heated to 120 °C for ~12 hrs. After this time the mixture was cooled to room temperature and the resulting residue was purified by silica gel chromatography eluting with

EtOAc:MeOH (95:5) to give the desired product as a white solid (0.033 g, 36%); δ H (500 MHz, MeOD) 8.00 (s, 1H), 7.40 (d, J = 8.3 Hz, 2H), 7.35 (d, J = 8.6 Hz, 2H), 6.10 (d, J = 7.5 Hz, 1H), 4.79 (dd, J = 7.6, 5.4 Hz, 1H), 4.66 (d, J = 15.9 Hz, 1H), 4.62 (d, J = 16.0 Hz, 1H), 4.30 (dd, J = 5.4, 1.7 Hz, 1H), 4.18 (q, J = 1.9 Hz, 1H), 3.85 (dd, J = 11.9, 2.3 Hz, 1H), 3.79 (dd, J = 12.0, 1.7 Hz, 1H); δ C (126 MHz, MeOD) 152.19, 151.83, 149.68, 148.72, 137.67, 132.42, 128.22, 128.16, 116.54, 87.30, 86.40, 71.65, 71.50, 61.73, 44.80; HRMS (ESI) $C_{17}H_{20}ClN_6O_4$ ($M+H^+$) requires 407.1229, found 407.1237.

(2R,3R,4S,5R)-2-(6-amino-8-((4-fluorobenzyl)amino)-9H-purin-9-yl)-5-(hydroxymethyl)tetrahydrofuran-3,4-diol 19

To a solution of 8-bromoadenosine (0.048 g, 0.139 mmol) in *n*-butanol (1.387 ml) was added (4-fluorophenyl)methanamine (0.032 ml, 0.277 mmol) and iPr_2NEt (0.073 ml, 0.416 mmol) and the mixture was heated to 120 °C ON. After this time the mixture was cooled to room temperature and the solvent removed under reduced pressure. The resulting residue was purified by silica gel chromatography eluting with EtOAc:MeOH (9:1) to give the desired product as a white solid (0.043 g, 79%); δ H (500 MHz, MeOD) 7.50 (dd, J = 8.3, 5.3 Hz, 1H), 7.44 - 7.38 (m, 2H), 7.23 - 7.16 (m, 1H), 7.09 - 7.04 (m, 2H), 6.09 (d, J = 7.6 Hz, 1H), 4.78 (dd, J = 7.6, 5.4 Hz, 1H), 4.65 (d, J = 15.7 Hz, 1H), 4.60 (d, J = 15.7 Hz, 1H), 4.29 (dd, J = 5.4, 1.6 Hz, 1H), 4.17 (q, J = 1.9 Hz, 1H), 3.83 (dd, J = 12.0, 2.2 Hz, 1H), 3.78 (dd, J = 11.9, 1.7 Hz, 1H); δ C (126 MHz, MeOD) 164.14, 163.00, 161.06, 152.14, 151.85, 149.66, 148.65, 134.75, 134.72, 130.99, 130.92, 128.53, 128.46, 116.55, 115.67, 115.50, 114.79, 114.62, 87.26, 86.41, 71.60, 71.50, 61.72, 44.79;³⁹ HRMS (ESI) $C_{17}H_{20}FN_6O_4$ ($M+H^+$) requires 391.1525, found 391.1517.

(2R,3R,4S,5R)-2-(6-amino-8-((4-methylbenzyl)amino)-9H-purin-9-yl)-5-(hydroxymethyl)tetrahydrofuran-3,4-diol 20

To a solution of 8-bromoadenosine (0.062 g, 0.179 mmol) in *n*-butanol (1.791 ml) was added *p*-tolylmethanamine (0.045 ml, 0.358 mmol) and ⁱPr₂NEt (0.093 ml, 0.537 mmol) and the mixture was heated to 120 °C for ~48 hrs. After this time the mixture was cooled to room temperature and the solvent removed under reduced pressure. The resulting residue was purified by silica gel chromatography eluting with EtOAc:MeOH (9:1) to give the desired product as a white solid (0.042 g, 60.7%); δH (500 MHz, MeOD) 7.99 (s, 1H), 7.28 (d, *J* = 7.8 Hz, 2H), 7.16 (d, *J* = 7.7 Hz, 2H), 6.09 (d, *J* = 7.6 Hz, 1H), 4.80 (dd, *J* = 7.6, 5.4 Hz, 1H), 4.64 (d, *J* = 15.6 Hz, 1H), 4.58 (d, *J* = 15.6 Hz, 1H), 4.29 (dd, *J* = 5.4, 1.7 Hz, 1H), 4.18 (d, *J* = 1.9 Hz, 1H), 3.84 (dd, *J* = 12.0, 2.3 Hz, 1H), 3.78 (dd, *J* = 11.9, 1.7 Hz, 1H), 2.32 (s, 3H); δC (126 MHz, MeOD) 152.08, 152.01, 149.64, 148.59, 136.39, 135.64, 128.70, 126.57, 116.57, 87.27, 86.40, 71.61, 71.50, 61.74, 45.26; HRMS (ESI) C₁₈H₂₃N₆O₄ (M+H⁺) requires 387.1775, found 387.1779.

(2R,3R,4S,5R)-2-(6-amino-8-((3,4-dichlorobenzyl)amino)-9H-purin-9-yl)-5-(hydroxymethyl)tetrahydrofuran-3,4-diol 21

To a microwave vial was added 8-bromoadenosine (0.300 g, 0.870 mmol) and 3,4-dichlorobenzylamine (0.29 ml, 2.17 mmol) in ethanol (1.73 ml). The reaction mixture was irradiated at 140 °C for 90 min. The reaction mixture was concentrated and the crude residue was purified by silica gel column chromatography eluting with EtOH:DCM (3:7) to give the desired product as a white solid (0.28 g, 73%); δH (500 MHz, DMSO-d₆) 7.90 (s, 1H), 7.70 – 7.53 (m, 3H), 7.37 (dd, *J* = 8.3, 2.0 Hz, 1H), 6.55 (s, 2H), 5.99 – 5.85 (m, 2H), 5.32 (d, *J* = 6.6 Hz, 1H), 5.18 (d, *J* = 4.0 Hz, 1H), 4.72 (td, *J* = 7.0, 5.3 Hz, 1H), 4.56 (d, *J* = 6.0 Hz, 2H), 4.12 (ddd, *J* = 5.5, 3.9, 1.9 Hz, 1H), 3.99 (q, *J* = 2.3 Hz, 1H), 3.62 (dt, *J* = 7.0, 3.2 Hz, 2H); δC (126 MHz, DMSO-d₆) 153.0, 151.5, 150.3, 149.2, 141.7, 131.3, 130.9, 129.7, 129.6, 128.1, 117.4, 87.0,

86.30, 71.5, 71.4, 62.2, 44.8; HRMS (ESI) C₁₇H₁₉Cl₂N₆O₄ (M+H⁺) requires 442.0867, found 442.0859.

(2R,3R,4S,5R)-2-(6-amino-8-((4-methoxybenzyl)amino)-9H-purin-9-yl)-5-(hydroxymethyl)tetrahydrofuran-3,4-diol 22

To a solution of 8-bromoadenosine (0.073 g, 0.211 mmol) in *n*-butanol (4.22 ml) was added (4-methoxyphenyl)methanamine (0.083 ml, 0.633 mmol) and iPr₂NEt (0.221 ml, 1.265 mmol) and the mixture was heated to 120 °C for ~12 hrs. After this time the mixture was cooled to room temperature and the solvent removed under reduced pressure. The resulting residue was purified by silica gel chromatography eluting with EtOAc:MeOH (95:5) to give the desired product as a white solid (0.049 g, 58%); δH (500 MHz, MeOD) 7.98 (s, 1H), 7.32 (d, *J* = 8.8 Hz, 1H), 6.89 (d, *J* = 8.8 Hz, 1H), 6.07 (d, *J* = 7.6 Hz, 1H), 4.78 (dd, *J* = 7.6, 5.4 Hz, 1H), 4.60 (d, *J* = 15.3 Hz, 1H), 4.55 (d, *J* = 15.3 Hz, 1H), 4.28 (dd, *J* = 5.6, 1.7 Hz, 1H), 4.16 (q, *J* = 1.9 Hz, 1H), 3.83 (dd, *J* = 12.0, 2.3 Hz, 1H), 3.78 (s, 3H), 3.77 (obs. dd, *J* = 11.9, 1.7 Hz, 1H); δC (126 MHz, MeOD) 158.96, 152.09, 151.98, 149.63, 148.59, 130.63, 127.94, 116.59, 113.49, 87.27, 86.38, 71.61, 71.48, 61.73, 54.26, 45.05; HRMS (ESI) C₁₈H₂₂N₆NaO₅ (M+Na⁺) requires 425.1544, found 425.1540.

Experimental Procedures (Surface Plasmon Resonance Spectroscopy)

Experimental Procedure (X-ray Crystallography)

ACKNOWLEDGMENT

(Word Style “TD_Acknowledgments”). Generally the last paragraph of the paper is the place to acknowledge people, organizations, and financing (you may state grant numbers and sponsors here). Follow the journal’s guidelines on what to include in the Acknowledgments section.

ABBREVIATIONS

HSP70, Heat Shock Protein 70; HSP72, Heat Shock Protein 72; HSC70, Heat Shock Cognate 70; tr-, truncated; ATP, adenosine triphosphate; ADP, adenosine diphosphate; P_i, inorganic phosphate; K_D, equilibrium dissociation constant; pK_D, Log of the equilibrium dissociation constant; SEM, standard error of the mean; μM, micromolar; n, number of statistical repeats; NBD, nucleotide binding domain; SPR, surface plasmon resonance.

1 Hartl, F. U.; Bracher, A.; Hayer-Hartl, M. Molecular chaperones in protein folding and proteostasis. *Nature* **2011**, *475*, 324.

2 Powers, M. V.; Workman, P. Inhibitors of the heat shock response: Biology and pharmacology. *FEBS Lett.* **2007**, *581*, 19, 3758-3769.

3 Pacey, S.; Banerji, U.; Judson, I.; Workman, P. HSP90 inhibitors in the clinic. *Handbook Exp. Pharm.* **2006**, *172*, 331-358.

4 Powers, M. V.; Jones, K.; Barillari, C.; Westwood, I.; van Montfort, R. L. M.; Workman, P. Targeting HSP70: the second potentially druggable heat shock protein and molecular chaperone? *Cell Cycle*, **2010**, *9*, 8, 1542-1550.

5 Powers, M. V.; Clarke, P. A.; Workman, P. Dual targeting of HSC70 and HSP72 inhibits HSP90 function and induces tumor-specific apoptosis. *Cancer Cell* **2008**, *14*, 3, 250-262.

6 (a) Mayer, M. P.; Bukau, B. HSP70 chaperones: Cellular functions and molecular mechanism. *Cellular Mol. Life Sci.* 2005, 62, 6, 670-684. (b) Laufen, T.; Mayer, M. P.; Beisel, C.; Klostermeier, D.; Mogk, A.; Reinstein, J.; Bukau, B. Mechanism of regulation of Hsp70 chaperones by DnaJ cochaperones. *Proc. Nat. Acad. Sci. Int. Ed.* **1999**, 96, 10, 5442-5457.

7 (a) Williamson, D. S.; Borgognoni, J.; Clay, A.; Daniels, Z.; Dokurno, P.; Drysdale, M. J.; Foloppe, N.; Francis, G. L.; Graham, C. J.; Howes, R.; Macias, A. T.; Murray, J. B.; Parsons, R.; Shaw, T.; Surgenor, A. E.; Terry, L.; Wang, Y.; Wood, M.; Massey, A. J. Novel Adenosine-Derived Inhibitors of 70 KDa Heat Shock Protein, Discovered Through Structure-Based Design. *J. Med. Chem.* **2009**, 52, 1510-1513. (b) Macias, A. T.; Williamson, D. S.; Allen, N.; Borgognoni, J.; Clay, A.; Daniels, Z.; Dokurno, P.; Drysdale, M. J.; Francis, G. L.; Graham, C. J.; Howes, R.; Matassova, N.; Murray, J. B.; Parsons, R.; Shaw, T.; Surgenor, A. E.; Terry, L.; Wang, Y.; Wood, M.; Massey, A. J. Adenosine-Derived Inhibitors of 78 KDa Glucose Regulated Protein (Grp78) ATPase: Insights into Isoform Selectivity. *J. Med. Chem.* **2011**, 54, 4034-4041.

8 Several non-ATP competitive inhibitors have been described in the literature see: (a) Fewell, S. W.; Day, B. W.; Brodsky, J. L. Identification of an Inhibitor of hsc70-mediated Protein Translocation and ATP Hydrolysis. *J. Biol. Chem.* **2001**, 276, 910-914. (b) Fewell, S. W.; Smith, C. M.; Lyon, M. A.; Dumitrescu, T. P.; Wipf, P.; Day, W. W.; Brodsky, J. L. Small Molecule Modulators of Endogenous and Co-chaperone stimulated Hsp70 ATPase Activity. *J. Biol. Chem.* **2004**, 279, 51131-51140. (c) Rousaki, A.; Miyata, Y.; Jinwal, U. K.; Dickey, C. A.; Gestwicki, J. E.; Zuiderweg, E. R. Allosteric drugs: the interaction of antitumor compound MKT-077 with human Hsp70 chaperones. *J. Mol. Biol.* **2011**, 411, 3, 614-632. (d) Williams, D. R.; Ko, S. K.; Park, S.; Lee, M. R.; Shin, I. An apoptosis-inducing small molecule that binds to heat shock

protein 70. *Angew. Chem. Int. Ed. Engl.* **2008**, *47*, 39, 7466-7469. (e) Jinwal, U. K.; Miyata, Y.; Koren, J.; Jones, J. R.; Trotter, J. H.; Chang, L.; O'Leary, J.; Morgan, D.; Lee, D. C.; Shults, C. L.; Rousaki, A.; Weeber, E. J.; Zuiderweg, E. R. P.; Gestwicki, J. E.; Dickey, C. A. Chemical Manipulation of Hsp70 ATPase Activity Regulates Tau Stability. *J. Neuroscience* **2009**, *29*, 39, 12079-12088. (f) Miyata, Y.; Rauch, J. N.; Jinwal, U. K.; Thompson, A. D.; Sharan Srinivasan, S.; Dickey, C. A.; Gestwicki, J. E. Cysteine Reactivity Distinguishes Redox Sensing by the Heat Inducible and Constitutive Forms of Heat Shock Protein 70 (Hsp70). *Chem. Biol.* **2012**, *19*, 11, 1391–1399. (g) Howe, M. K.; Bodoor, K.; Carlson, D. A.; Hughes, P. F.; Alwarawrah, Y.; Loiselle, D. R.; Jaeger, A. M.; Darr, D. B.; Jordan, J. L.; Hunter, L. M.; Molzberger, E. T.; Gobillot, T. A.; Thiele, D. J.; Brodsky, J. L.; Spector, N. L.; Haystead, T. A. J. Identification of an Allosteric Small-Molecule Inhibitor Selective for the Inducible Form of Heat Shock Protein 70. *Chem. Biol.* **2014**, *21*, 1-12. (h) Dal Piaz, F.; Cotugno, R.; Lepore, L.; Vassallo, A.; Malafrente, N.; Lauro, G.; Bifulco, G.; Belisario M. A.; De Tommasi, N. Chemical proteomics reveals HSP70 1A as a target for the anticancer diterpene oridonin in Jurkat cells. *J. Proteomics* **2013**, *82*, 14-26. (i) Rodina, A.; Patel, P. D.; Kang, Y.; Patel, Y.; Baaklini, I.; Wong, M. J.; Taldone, T.; Yan, P.; Yang, C.; Maharaj, R.; Gozman, A.; Patel, M. R.; Patel, H. J.; Chirico, W.; Erdjument-Bromage, H.; Talele, T. T.; Young, J. C.; Chiosis, G. Identification of an allosteric pocket on human hsp70 reveals a mode of inhibition of this therapeutically important protein. *Chem. Biol.* **2013**, *20*, 12, 1469-1480.

9 (a) Bork, P.; Sander, C.; Valencia, A. An ATPase domain common to prokaryotic cell cycle proteins, sugar kinases, actin, and HSP70 heat shock proteins. *Proc. Natl. Acad. Sci. USA* **1992**, *89*, 7290-7294. (b) Flaherty, K. M.; McKay, D. B.; Kabsch, W.; Holmes, K. Similarity of the

three-dimensional structures of actin and the ATPase fragment of a 70-kDa heat shock cognate protein. *Proc. Natl. Acad. Sci. USA* **1991**, *88*, 5041-5045. (c) Chene, P.; ATPases as Drug Targets: Learning from their Structure. *Nat. Rev. Drug Disc.* **2002**, *1*, 665-673.

10 Massey, A. J. ATPases as Drug Targets: Insights from Heat Shock Proteins 70 and 90. *J. Med. Chem.* **2010**, *53*, 7280–7286.

11 SiteMap, version 2.2; Schrodinger LLC (120 West 45th Street, New York, NY 10036), 2008.

12 HSP70 is quoted as returning a Dscore 0.95 classifying the target as “difficult”, see reference 10 and Halgren, T. A. Identifying and characterizing binding sites and assessing drugability. *J. Chem. Inf. Model.* **2009**, *49*, 377–389.

13 This analysis was carried out by Vernalis using their fragment screening deck, see reference 10 and Hajduk, P. J.; Huth, J. R.; Fesik, S. W. Drugability indices for protein targets derived from NMR-based screening data. *J. Med. Chem.* **2005**, *48*, 7, 2518–2525.

14 (a) Arakawa, A.; Handa, N.; Ohsawa, N.; Shida, M.; Kigawa, T.; Hayashi, F.; Shirouzu, M.; Yokoyama, S. The C-Terminal BAG Domain of BAG5 Induces Conformational Changes of the Hsp70 Nucleotide-Binding Domain for ADP-ATP Exchange. *Structure* **2010**, *18*, 309-319. (b) Vogel, M.; Bukau, B.; Mayer, M. P. Allosteric Regulation of Hsp70 Chaperones by a Proline Switch. *Mol. Cell* **2006**, *21*, 359-367. (c) Rist, W.; Graf, C.; Bukau, B.; Mayer, M. P. Amide Hydrogen Exchange Reveals Conformational Changes in Hsp70 Chaperones Important for Allosteric Regulation. *J. Bio. Chem.* **2006**, *281*, 24, 16493-16501. (d) Mayer, M. P.; Bukau, B.

Hsp70 chaperones: Cellular functions and molecular mechanism. *Cell. Mol. Life Sci.* **2005**, *62*, 670–684.

¹⁵ The off-rate of ADP/P_i from HSP72 has been calculated using MABA-ADP and is $\sim 0.05 \text{ s}^{-1}$, the steady state ATPase rate in the absence of co-chaperones has been calculated as $\sim 4.5 \times 10^{-4} \text{ s}^{-1}$, see: Gassler, C. S.; Wiederkehr, T.; Brehmer, D.; Bukau, B.; Mayer, M. P. Bag-1M Accelerates Nucleotide Release for Human Hsc70 and Hsp70 and Can Act Concentration-dependent as Positive and Negative Cofactor. *J. Bio. Chem.* **2001**, *276*, 35, 32538-32544.

¹⁶ For more details see the supporting information.

¹⁷ All SPR data was measured with the Biacore T200 instrument using the analysis software (Version 2) provided. tr-HSC70 was loaded on to the Series S CM5 sensor chip as per the manufactures instructions and in the presence of 750 μM ADP to protect active site lysines. $\text{pK}_D = -\log_{10}[\text{K}_D(\mu\text{M}) \cdot 10^{-6}]$. All results are the geometric mean \pm SEM of three independent experiments measured at similar protein binding levels ($\sim 5000 \text{ RU}$). The K_D values were determined from analysis of the background normalized binding curve generated from the sensorgrams under equilibrium conditions using a 1:1 binding model. For all experiments, the ratio of experimental RU_{max} to theoretical RU_{max} was approximately 1. Representative examples of sensorgrams and binding curves can be found in the supporting information.

¹⁸ Standard adenosine and adenine numbering system is used throughout this publication.

¹⁹ This data can be observed in the supplementary information.

²⁰ All fold differences that are quoted are statistically significant at the 95% level using Student's t-test, see: Cumming, G.; Fidler, F.; Vaux, D. L. Error bars in experimental biology. *J. Cell Bio.* **2007**, *177*, 1, 7-11.

²¹ Stumpfe, D.; Hu, Y.; Dimova, D.; Bajorath, J. Recent Progress in Understanding Activity Cliffs and Their Utility in Medicinal Chemistry. *J. Med. Chem.* **2014**, *57*, 1, 18-28.

²² See supporting information for purchasing details of commercially available natural products used in this study.

²³ Gunic, E.; Girardet, J.; Pietrkowski, Z.; Esler, C.; Wang, G. Synthesis and Cytotoxicity of 4'-C- and 5'-C-Substituted Toyocamycins. *Bioorg. Med. Chem.* **2001**, *9*, 163-170.

²⁴ 8-*N*-Methylaminosangivamycin could only be isolated in 80% purity and was tested at this level of purity in subsequent assays.

²⁵ Due to the low yield and purity in the synthesis **13** there was only sufficient material to do a single SPR analysis to measure the compound's affinity to HSP70.

²⁶ Kuhn, B.; Mohr, P.; Stahl, M.; Intramolecular Hydrogen Bonding in Medicinal Chemistry. *J. Med. Chem.* **2010**, *53*, 6, 2601–2611.

²⁷ Minamoto, K.; Fujiki, Y.; Shiomi, N.; Uda, Y.; Sasaki, T. Systematic General Synthesis of Purine 8,5'-Imino and Substituted Imino Cyclonucleosides. *J. Chem. Soc. Perkin Trans. 1: Org. Bioorg. Chem.* **1985**, *11*, 2337-2346.

²⁸ Ha, J.; McKay, D. B. Kinetics of Nucleotide-Induced Changes in the Tryptophan Fluorescence of the Molecular Chaperone Hsc70 and Its Subfragments Suggest the ATP-Induced Conformational Change Follows Initial ATP Binding. *Biochem.* **1995**, *34*, 11635-11644.

²⁹ For a discussion on the effect of binding mechanism and conformational change in drug discovery see: Holdgate, G. A.; Gill, A. L. Kinetic efficiency: the missing metric for enhancing compound quality? *Drug Disc. Today* **2011**, *16*, 910-913.

³⁰ Danley, D. E. Crystallization to obtain protein-ligand complexes for structure-aided drug design. *Acta Crystallogr. D: Biol. Crystallogr.* **2006**, *6*, 569-575.

³¹ This result is comparable to the previously described affinity ADP for HSP70 ($K_D = 0.5 \mu\text{M}$). See reference 7. The affinity of ADP for HSP70 is known to be highly dependent on the assay conditions, see: Arakawa, A.; Handa, N.; Ahirouzu, M.; Yokoyama, S. Biochemical and structural studies on the high affinity of HSP70 for ADP. *Protein Sci.* **2011**, *20*, 1367-1379.

³² The salt-bridge between glutamic acid-268 and lysine-56 can be observed in several other published HSP70/ADP structures, see: (a) PDB 3ATU reference 31; (b) PDB 3JXU Wisniewska, M.; Karlberg, T.; Lehtio, L.; Johansson, I.; Kotenyova, T.; Moche, M.; Schuler, H.; Crystal Structures of the ATPase Domains of Four Human Hsp70 Isoforms: HSPA1L/Hsp70-hom, HSPA2/Hsp70-2, HSPA6/Hsp70B', and HSPA5/BiP/GRP78. *PLoS ONE* **2010**, *5*, 1, e8625, 1-8; (c) PDB 1S3X Sriram, M.; Osipiuk, J.; Freeman, B.; Morimoto, R.; Joachimiak, A. Human Hsp70 molecular chaperone binds two calcium ions within the ATPase domain. *Structure* **1997**, *15*, 5, 3, 403-414;

³³ Rye, C. S.; Baell, J. B. Phosphate isosteres in medicinal chemistry. *Curr. Med. Chem.* **2005**, *12*, 26, 3127-3141.

³⁴ 8-*N*-quinolineaminoadenosine derived ligand **17** was previously reported to have a $K_D = 0.23 \mu\text{M}$ as measured by SPR against the HSP70 isoform GRP78, see reference 7.

³⁵ (a) Luo, R.; David, L.; Hung, H.; Devaney, J.; Gilson, M. K. Strength of Solvent-Exposed Salt-Bridges. *J. Phys. Chem. B* **1999**, *103*, 4, 727-736. (b) Dong, F.; Zhou, H. Electrostatic Contributions to T4 Lysozyme Stability: Solvent-Exposed Charges versus Semi-Buried Salt Bridges. *Biophys. J.* **2002**, *83*, 1341-1347.

³⁶ Berry, B. W.; Elvekrog, M. M.; Tommos, C. Environmental Modulation of Protein Cation- π Interactions. *J. Am. Chem. Soc.* **2007**, *129*, 17, 5308-5309.

³⁷ For a discussion on the effects of "burying" solvent exposed intramolecular hydrogen bonds and salt-bridges of proteins, see: (a) Hendsch, Z. S.; Tidor, B. Do salt bridges stabilize proteins? A continuum electrostatic analysis. *Protein Sci.* **1994**, *3*, 211-226. (b) Efimov, A.; Brazhnikov, E. V.; Relationship between intramolecular hydrogen bonding and solvent accessibility of side-chain donors and acceptors in proteins. *FEBS Lett.* **2003**, *554*, 389-393.

³⁸ (a) Porcari, A. R.; Townsend, L. B.; *Synth. Commun.* **1998**, *28*, 3835-3843; Dang, Q.; Gomez-Galeno, J. E.; *J. Org. Chem.* **2002**, *67*, 8703-8705; (b) Taylor, E. C.; Hendess, R. W.; *J. Am. Chem. Soc.* **1965**, *87*, 1995-2003; (c) Sharma, M.; Bloch, A.; Bobek, M.; *Nucleosides & Nucleotides*, **1993**, *12*(6), 643-8.

³⁹ Complex due to F-coupling.